Adsorption 7, 51–63, 2001
© 2001 Kluwer Academic Publishers. Manufactured in The Netherlands.

# Discrimination of Adsorption Kinetic Models for the Description of Hydrocarbon Adsorption in Activated Carbon

K. WANG, S. QIAO AND X. HU
*Department of Chemical Engineering, Hong Kong University of Science and Technology, Clear Water Bay, Hong Kong*

D.D. DO*
*Department of Chemical Engineering, The University of Queensland, Brisbane, QLD 4072, Australia*
duongd@cheque.uq.edu.au

*Received May 4, 2000; Revised October 23, 2000; Accepted November 6, 2000*

**Abstract.** Five kinetic models for adsorption of hydrocarbons on activated carbon are compared and investigated in this study. These models assume different mass transfer mechanisms within the porous carbon particle. They are: (a) dual pore and surface diffusion (MSD), (b) macropore, surface, and micropore diffusion (MSMD), (c) macropore, surface and finite mass exchange (FK), (d) finite mass exchange (LK), and (e) macropore, micropore diffusion (BM) models. These models are discriminated using the single component kinetic data of ethane and propane as well as the multicomponent kinetics data of their binary mixtures measured on two commercial activated carbon samples (Ajax and Norit) under various conditions. The adsorption energetic heterogeneity is considered for all models to account for the system. It is found that, in general, the models assuming diffusion flux of adsorbed phase along the particle scale give better description of the kinetic data.

**Keywords:** adsorption, kinetics, modelling, activated carbon

## Introduction

The structure of activated carbon (AC) is generally bidispersed, consisting of graphite crystals (microparticles or grains) distributed randomly within a maze of amorphous carbons. The former accommodates the microporous network which accounts for most of the adsorption capacity (and the selectivity for multicomponent systems) while the latter provides the transport channels into the particle. Since the surface area of commercial AC is normally very high ($\sim$1,000 $m^2/g$), the diffusion of the adsorbed phase along the particle scale, or the surface diffusion, can make a significant contribution to the overall mass transfer for strongly adsorbed species. This diffusion mechanism has been verified with a number of experimental techniques, such as gas permeation (Do, 1997), kinetics uptake measurement (Ruthven, 1984; Karger, 1988), and Wicke-Kallenbach method (Kapoor and Yang, 1991), etc. However, because of the complexity in the microscopic structure of AC, the mechanism of surface diffusion remains a topic for debate as there are also studies suggesting that surface diffusion only occurs in the microparticle (grain) scale. Effort trying to incorporate these two different approaches is also seen in the literature, as Bhatia proposed that the flux of the adsorbed species along particle scale should be related to the diffusion flux on microparticle scale (Bhatia, 1997). The physical picture for surface diffusion in the highly random 3-D space of AC is not yet clear, but it has been viewed as a process involving adsorption into and

*To whom all correspondence should be addressed.

evaporation from the microparticle units (Do, 1996), or hopping between neighboring adsorption sites (Kapoor et al., 1989). To further complicate this issue, the surface flux in an AC always parallels with other transport fluxes (such as bulk diffusion or viscous flow). As a result, models assuming different mechanisms for surface diffusion may possess similar capabilities (within experimental error) in simulating a range of experimental data. Therefore, to discriminate among various mathematical models for adsorption kinetics in AC, experimental data measured at various experimental conditions may be necessary.

The differential adsorption bed (DAB) rig has been proved to be a reliable experimental technique for studying sorption kinetics of pure gas as well as gaseous mixtures. It has the advantage of measuring the uptake (adsorbed phase concentration) directly while keeping a constant boundary conditions at the external surface of adsorbent particles. Due to the very high gas flow around the adsorbent particles (>3,000 cc/g/min), the isothermality is mostly satisfied in the DAB technique. However, DAB has the disadvantage of being extremely time-consuming that tremendous effort is needed if sorption kinetics of a system are to be collected at various experimental conditions. In the past few years, Do and Hu have systematically collected the sorption kinetic data on two commercial AC samples (Ajax and Norit AC) with DAB technique. Sorption kinetics of pure gas as well as gas mixtures were collected over a range of temperatures, bulk phase compositions as well as on particles with different sizes and geometries. These extensive experimental data are employed in this article to discriminate various kinetic models assuming different mass transfer mechanisms.

## Theories

In spite of the bidispersed nature, the microscopic structure of AC is very complicated and presents strong energetic heterogeneity towards adsorption, and such heterogeneity must be accounted for in any kinetic model to correctly describe adsorption kinetics (Do, 1997). A common approach is to assume a patchwise surface (Kapoor and Yang, 1991) for sorption equilibria and a parallel path model or PPM (Kapoor and Yang, 1989) for sorption kinetics. These approaches, although being oversimplified for a real carbon surface, address the heterogeneity in a fundamental manner yet the keeping the model simple enough for practical applications. Other approaches like effective media approach (EMA) (Kapoor and Yang, 1989) or pore network model (Mann and Yousef, 1995) might describe the reality a bit better but are mathematically more complicated. Thus, to fully demonstrate and compare the capabilities of various kinetics models in describing sorption kinetics, the energetic heterogeneity is considered in this study.

In this study, the flux of bulk phase diffusion along the particle coordinate, $R$, is described by the Fick's law:

$$J_{\mathrm{P}} = -D_{\mathrm{P}} \frac{\partial C}{\partial R} \tag{1}$$

where the pore diffusivity, $D_{\mathrm{p}}$, is the combination of the Knudsen and molecular diffusivities (Ruthven, 1984).

The driving force for surface diffusion is taken as the gradient of chemical potential ($\mu$) and the surface flux of a pure component system on a patch with an interaction energy $E$ is:

$$\begin{aligned} J_\mu(E) &= -L_\mu(E) C_\mu(E) \frac{\partial \mu}{\partial R} \\ &= -D_\mu(E) \frac{\partial \ln C}{\partial \ln C_\mu(E)} \frac{\partial C_\mu(E)}{\partial R}. \end{aligned} \tag{2a}$$

Equation (2a) delineates the surface flux along the particle scale. On microparticle scale, $r$, the surface flux is written as:

$$J^r_\mu(E) = -D_\mu(E) C_\mu(E) \frac{\partial \mu}{\partial r} \tag{2b}$$

where $D_\mu(E)$ is the surface diffusivity at zero loading. The use of chemical potential as driving force invokes the 'thermodynamics correction factor' (the term, $\partial \ln C_\mu / \partial \ln C$, in Eq. (2a)) for surface diffusivity. Surface diffusion has been known to be an activation process and follows an Arrhenius type temperature dependence (Kapoor et al., 1989):

$$D_\mu(E) = D^0_\mu \exp(-E_a / R_g T) \tag{3a}$$

where $D^0_\mu$ is the surface diffusivity at zero energy level and $E_{\mathrm{a}}$ is the activation energy for surface diffusion. $E_{\mathrm{a}}$ is related to the interaction energy, $E$, as follows:

$$E_a = a \times E \tag{3b}$$

where '$a$' has been reported to take the value between 0.3 to 1 for physical adsorption processes (Kapoor et al., 1989). It has been found experimentally by Prasetyo and Do that it takes the value of 0.5 and 0.6

for ethane and propane, respectively (Prasetyo and Do, 1999).

The above theories are generally accepted for adsorption and diffusion processes and are used in our kinetic models, where applicable.

Five models with different mass transfer mechanisms are investigated in this article. To save space, only equations for single component systems are presented here. These models are:

### 1. *Macropore and Surface Diffusion Model*

The macropore and surface diffusion (MSD) model is proposed for adsorption on large-sized AC particles, in which the diffusion resistance along the microparticle scale is negligible and local equilibrium is assumed between the two phases (Do et al., 1991). The mass balance over *an energy patch* in a particle with the geometric factor of '*s*' (0, 1, 2 for slab, cylinder, and sphere, respectively) is written as:

$$\varepsilon\frac{\partial C}{\partial t}+(1-\varepsilon)\frac{\partial C_\mu(E)}{\partial t} = -\frac{1}{R^s}\frac{\partial}{\partial R}[\varepsilon R^s J_{\mathrm{P}}+(1-\varepsilon)\times R^s J_\mu(E)] \quad (4)$$

where $\varepsilon$ is the macroporosity of the particle. Since the bulk and the adsorbed phases are in local equilibrium, the driving force for surface diffusion equals the gradient of chemical potential, $\mu$ in the bulk phase. In this case, Eq. (2a) will suggest a Darken type relation for the concentration dependence of the 'apparent' surface diffusivity if the Langmuir isotherm is employed. The kinetic parameter to be studied in this model is the surface diffusivity, $D_\mu$.

### 2. *Bimodal Diffusion Model*

The bimodal diffusion (BM) model has been used successfully for sorption kinetics in adsorbents like zeolite pellets composing of zeolite crystals. Mass transfer resistance is described by macropore diffusion along the pellet scale as well as micropore diffusion along the crystal scale (Ruthven, 1984; Gray and Do, 1989). The mass balance equation for a patch with energy $E$ can be written as:

$$\varepsilon\frac{\partial C}{\partial t}+(1-\varepsilon)\frac{\partial C_\mu(E)}{\partial t}=\frac{1}{R^s}\frac{\partial}{\partial R}(\varepsilon R^s J_{\mathrm{P}}) \quad (5a)$$

and

$$\frac{\partial C_\mu(E)}{\partial t}=-\frac{1}{r^{s_u}}\frac{\partial}{\partial r}\left[r^{s_u}J_\mu^r(E)\right] \quad (5b)$$

where $r$ and $s_\mu$ are the scale and the geometric factor of a microparticle, respectively. The boundary condition at external surface of a microparticle is:

$$C_\mu(t, R, r_0, E) = f[C(t, R)] \quad (5c)$$

The unknown kinetic parameter in the BM is the diffusion time constant in the microparticle,

$$D_\mu^0/r_0^2.$$

### 3. *Macropore Surface Micropore Diffusion Model*

The macropore, surface and micropore diffusion (MSMD) model (Hu and Do, 1993) was developed for sorption kinetics on small-sized AC pellets in which the diffusion resistance along both the microparticle and particle scales are significant. The model takes that the diffusion into microparticle is more restricted and the diffusivity is different from that along the particle scale by a factor of $\beta^2$ ($\beta<1$). The MSMD model can be expressed as:

$$\frac{\partial}{\partial t}[\varepsilon C+(1-\varepsilon)C_\mu(E)] = -\frac{1}{R^s}\frac{\partial}{\partial R}[\varepsilon R^s J_P+(1-\varepsilon)\times R^s J_\mu(E)] \quad (6a)$$

with:

$$\frac{\partial C_\mu(E)}{\partial t}=-\frac{1}{r^{s_u}}\frac{\partial}{\partial r}\left[r^{s_u}J_\mu^r(E)\right] \quad (6b)$$

where $J_\mu^r(E)=\beta^2 J_\mu(E)$ is the diffusion flux along the microparticle scale. The boundary condition of Eq. (5c) is applicable for Eq. (6b). This model has two parameters to be determined: $D_\mu^0$ and $r_0/\beta$.

### 4. *Finite Kinetics Model*

The finite kinetics (FK) model interprets the mass transfer in AC by considering the structural characteristics of the adsorbent. It takes into account of the mass transfer resistances (such as the pore mouth resistance) between the bulk and the adsorbed phases so that three mass transfer processes (pore diffusion, surface diffusion and the finite interchange rate between the bulk

and adsorbed phases) occur (Do, 1996). With the finite mass interchange rate between the bulk and adsorbed phases being described by the Langmuir kinetics (Do and Wang, 1998), the mass balance is:

$$\frac{\partial}{\partial t}[\varepsilon C + (1-\varepsilon)C_\mu(E)] = -\frac{1}{R^s}\frac{\partial}{\partial R}[\varepsilon R^s J_P + (1-\varepsilon)\times R^s J_\mu(E)] \quad (7a)$$

and for the adsorbed phase it is:

$$\frac{\partial C_\mu(E)}{\partial t} = \frac{1}{R^s}\frac{\partial}{\partial R}[R^s J_\mu(E)] + k_a C[C_{\mu s} - C_\mu(E)] - k_{\rm d}(E)C_\mu(E) \quad (7b)$$

Because the adsorbed phase is not in local equilibrium with the gas phase within macropores, the surface flux equation has the form:

$$J_\mu(E) = -D_\mu(E)\frac{C_{\mu s}}{C_{\mu s} - C_\mu(E)}\frac{\partial C_\mu(E)}{\partial R} \quad (7c)$$

where $k_{\rm a}$ and $k_{\rm d}$ are the rate constants for adsorption and desorption, respectively. They are related to each other via the local adsorption affinity:

$$b(E) = k_{\rm a}/k_{\rm d}(E) \quad (7d)$$

The FK model has two kinetic parameters to be determined: $D_\mu^0$ and $k_{\rm a}$.

### 5. *Langmuir Kinetics Model*

The Langmuir kinetics (LK) model assumes that the mass transfer resistance in the entire adsorbent particle interior and periphery can be lumped into a shell resistance (Srinivasan et al., 1995). This model is applicable for sorption kinetics in molecular sieving carbon (CMS). Since in such adsorbent the resistance is not homogeneously distributed, the rate of adsorption and desorption are much slower than the rate of diffusion so that the overall uptake kinetics is dictated by the 'shell resistance'. This model works well in modeling $O_2/N_2$ mass transfer in CMS. LK model is a special case of FK in which the pore diffusion and surface diffusion terms in Eqs. (7) are removed.

$$\frac{\partial C_\mu}{\partial t} = k_{\rm a}C(C_{\mu s} - C_\mu) - k_{\rm d}C_\mu \quad (8)$$

The only unknown in this model is the rate constant of adsorption, $k_{\rm a}$.

### 6. *The Boundary Conditions*

The above five kinetic models are subject to boundary and initial conditions of the adsorption system. In a DAB rig, the bulk phase concentration at external surface can be regarded as being constant and in equilibrium with the adsorbed phase (Do, 1997). Thus, at the exterior surface of the particle we have:

$$\begin{aligned} &\text{at } t = 0, && C = 0 \\ &\text{at } t > 0, \text{ and } R = R_0 && C = C_0 \end{aligned} \quad (9)$$

### 7. *The Sorption Kinetics and Equilibria on a Heterogeneous Surface*

All five kinetics models are capable of incorporating the sorption energetic heterogeneity, but we shall only consider such incorporation for diffusion-based models because the performance of the LK model is inferior to the others, and therefore the extension of the LK model to account for heterogeneity is not warranted. A simple uniform energy distribution is assumed for the surface heterogeneity of AC samples in this study. With the maximum and minimum energy being $E_{\max}$ and $E_{\min}$, this distribution function takes the form of:

$$F(E) = \begin{cases} \dfrac{1}{E_{\max} - E_{\min}} & \text{for } E_{\min} < E < E_{\max} \\ 0 & \text{elsewhere} \end{cases} \quad (10)$$

Therefore, a heterogeneous isotherm is required to describe the adsorbed phase concentration during uptake. The MSD, BM, and MSMD models can take any form of isotherm. The other two kinetics models, i.e., FK and LK, require the Langmuir type isotherm due to their model assumptions on the mass transfer rate. To have an indentical basis for model comparison, a local Langmuir equation is employed for all kinetic models, i.e.

$$C_\mu(E) = C_{\mu s}\frac{b(E)C}{1 + b(E)C} \quad (11)$$

where $C_{\mu s}$ is the adsorption capacity. For LK model, the interaction energy $(E)$ is identical over the AC and the Eq. (11) reduces to the homogeneous Langmuir equation. The overall adsorbed phase concentration

and the diffusion flux on a heterogeneous surface can be expressed as:

$$C_\mu = \int_{E_{\min}}^{E_{\max}} C_\mu(E)F(E)\,dE \qquad (12a)$$

$$J_\mu = \int_{E_{\min}}^{E_{\max}} J_\mu(E)F(E)\,dE \qquad (12b)$$

That is, for a heterogeneous surface, Eqs. (12) suggests a patch-wise surface for equilibria [Eq. (12a)] and a parallel path model (PPM) for sorption kinetics [Eq. (12b)]. In this study, Eq. (12a) is the Unilan isotherm.

When a system contains more than one species, the local isotherm will take the form of extended Langmuir equation. The cumulative energy matching scheme is invoked to correlate the matching energies between different species in the adsorbed phase (Kapoor and Yang, 1989), that is:

$$\frac{E(i) - E(i)_{\min}}{E(i)_{\min} - E(i)_{\max}} = \frac{E(j) - E(j)_{\min}}{E(j)_{\min} - E(j)_{\max}} \qquad (13)$$

With Eqs. (10)–(13), four of the five kinetic models, i.e., MSD, BM, MSMD, FK, can be extended to multicomponent systems in a direct manner while the LK model only needs to incorporate the extended Langmuir equation. The detailed procedures of model development and the final forms of these model equations can be obtained from the literature (Do, 1997; Hu and Do, 1993; Do and Wang, 1998).

### *8. Model Solutions*

The four of the five kinetic models are in the forms of (partial) differential equations (PDE), which can be solved numerically with the orthogonal collocation technique combined with integration packages. The LK model is a simple ordinary differential equation (ODE). The detailed model solutions are available elsewhere (Do, 1997).

## Experiments

The adsorption kinetics of ethane and propane, as well as their binary mixtures were measured on Norit AC (Qiao and Hu, 1999), and Ajax AC (Do, 1997; Hu and Do, 1993) with DAB technique. The pure component adsorption equilibria of ethane and propane were measured with volumetric a rig. The experimental temperatures are selected as 10, 30, 60°C, for Ajax AC and 30, 60, 90°C for Norit AC, respectively. The sorption kinetic data on Ajax AC in 4.4 mm slabs and the kinetic data on Norit AC in 8.82 mm slab pellets were used in this study. The detailed experimental setup and procedures were described in Do (1997) and Qiao and Hu (1999). The physical properties of the two sample ACs and the experimental conditions for pure component equilibria and kinetics of the two adsorbates on each AC are listed in Table 1.

*Table 1.* The physical properties of the two sample ACs and the experimental parameters.

| | Density ($kg/m^3$) | Porosity | Surface area ($m^2/g$) | Experiment temperature (K) | Molar fraction (pure component, kinetics* of ethane and propane) |
|---|---|---|---|---|---|
| Ajax | 660 | 0.71 | 1200 | 10, 30, 60 | 5%, 10%, 20% |
| Norit | 569 | 0.74 | 1052 | 20, 60, 90 | 2%, 5%, 10% |

*Note: The kinetics at each molar fraction were measured for three temperatures.

## Results and Discussion

### *1. Adsorption Equilibrium and Energetic Heterogeneity*

The pure component equilibrium data of ethane and propane measured at multi-temperatures were employed to optimize the isotherm parameters for each species with Eq. (12a). The optimally obtained parameters are listed in Table 2 for ethane and Table 3 for propane, respectively. For LK model, the simple Langmuir equation was also used to fit the data at each temperature and the related parameters are also listed in Tables 2 and 3 (the last two columns) for ethane and propane, respectively.

It should be pointed out that, at the same temperature, the adsorption capacities, $C_{\mu s}$, of ethane and propane are constrained to be the same on each AC while deriving the isotherm parameters. This is designated to meet the thermodynamic consistency of the extended Langmuir isotherm equation which is used to describe multicomponent adsorption equilibria on each AC.

The information of equilibria and energetic heterogeneity will be used in the related kinetics models to simulate the sorption kinetics of each species.

*Table 2.* The isotherm parameters for ethane on the two AC samples.

| Sample | $T$ (K) | $C_{\mu s}$ (kmol/m$^3$) | $b_0$ (kPa$^{-1}$) | $E_{\min}$ (kJ/mol) | $E_{\max}$ (kJ/mol) | $C_{\mu s}$ (kmol/m$^3$) | $B$ (kPa$^{-1}$) |
|---|---|---|---|---|---|---|---|
| Norit | 303 | 4.76 | $1.50 \times 10^{-5}$ | 12.64 | 26.64 | 3.86 | 0.0559 |
| | 333 | 4.09 | | | | 3.32 | 0.0302 |
| | 363 | 3.53 | | | | 2.76 | 0.0167 |
| Ajax | 283 | 13.0 | $8.47 \times 10^{-7}$ | 6.26 | 30.75 | 5.29 | 0.0526 |
| | 303 | 13.0 | | | | 4.90 | 0.0360 |
| | 333 | 13.4 | | | | 4.58 | 0.0167 |

*Table 3.* The isotherm parameters for propane on the two AC samples.

| Sample | $T$ (K) | $C_{\mu s}$ (kmol/m$^3$) | $b_0$ (kPa$^{-1}$) | $E_{\min}$ (kJ/mol) | $E_{\max}$ (kJ/mol) | $C_{\mu s}$ (kmol/m$^3$) | $B$ (kPa$^{-1}$) |
|---|---|---|---|---|---|---|---|
| Norit | 303 | 4.76 | $2.77 \times 10^{-4}$ | 9.38 | 22.96 | 3.86 | 0.247 |
| | 333 | 4.09 | | | | 3.32 | 0.135 |
| | 363 | 3.53 | | | | 2.76 | 0.0815 |
| Ajax | 283 | 13.0 | $1.93 \times 10^{-7}$ | 0.0 | 42.75 | 5.29 | 0.448 |
| | 303 | 13.0 | | | | 4.90 | 0.197 |
| | 333 | 13.4 | | | | 4.58 | 0.0833 |

## 2. *Adsorption Kinetics of Pure Component Systems*

First, the five models are compared on the basis of their capabilities in fitting and simulating pure component sorption kinetics. The kinetics parameters in each model were derived by fitting the kinetic data of a species at one temperature but at several bulk phase concentrations. These parameters are then employed to predict the kinetics of this species at other temperatures (MSD, BM, MSMD, FK) or at other concentrations (LK). The goodness of fitting/simulation of each model are compared in terms of the average relative error (ARE), which is defined as:

$$\text{ARE} = \frac{100}{N} \sum_{k=1}^{N} \left| \frac{Y_{\text{model}} - Y_{\text{exp}}}{Y_{\text{exp}}} \right|_k \qquad (14)$$

where $N$ is the number of experimental data points and $Y$ is the fractional uptake.

For each model, the kinetic parameters of ethane and propane were derived with the following pure component kinetic data on each AC, they are, (1) Ajax AC, the kinetic data measured on 4.4 mm slab at 303 K with the molar fraction of 5%, 10%, 20%; (2) Norit AC, kinetic data measured on 8.82 mm slab at 303 K particle with the molar fraction of 2%, 5%, 10% (Qiao and Hu, 1999).

The derived kinetic parameters of ethane and propane on Ajax AC are listed in Tables 4 and 5 respectively, while those on Norit AC are listed in Tables 6 and 7, respectively. The ARE of the model fittings are also shown in the related tables. Also shown in the tables are the pore diffusivities used in the simulations for MSD, MSMD and FK models. Since the BM assumes the mechanism of micropore diffusion control, the pore diffusivity ($D_{\text{p}}$) is increased empirically to achieve the best fit of the experimental data.

We now consider the performance of each model in fitting the pure component kinetics of Ajax AC. Figure 1(a) shows the model fittings (lines) and the experimental data of ethane (symbols) on 4.4 mm slabs at the temperature of 303 K. Judging from the graph and the AREs listed in Table 4, we see that, MSD, MSMD, FK and LK models fit the data comparably well while BM presents a larger deviation. However, all the model fittings can be regarded as reasonable and it seems that the simplicity would be the primary factor in selecting a model in this case. Figure 1(b) shows the model fittings (lines) and the experimental data (symbols) of propane on 4.4 mm slab at 303 K and the ARE for the fittings are shown in Table 5. Similar trend is observed,

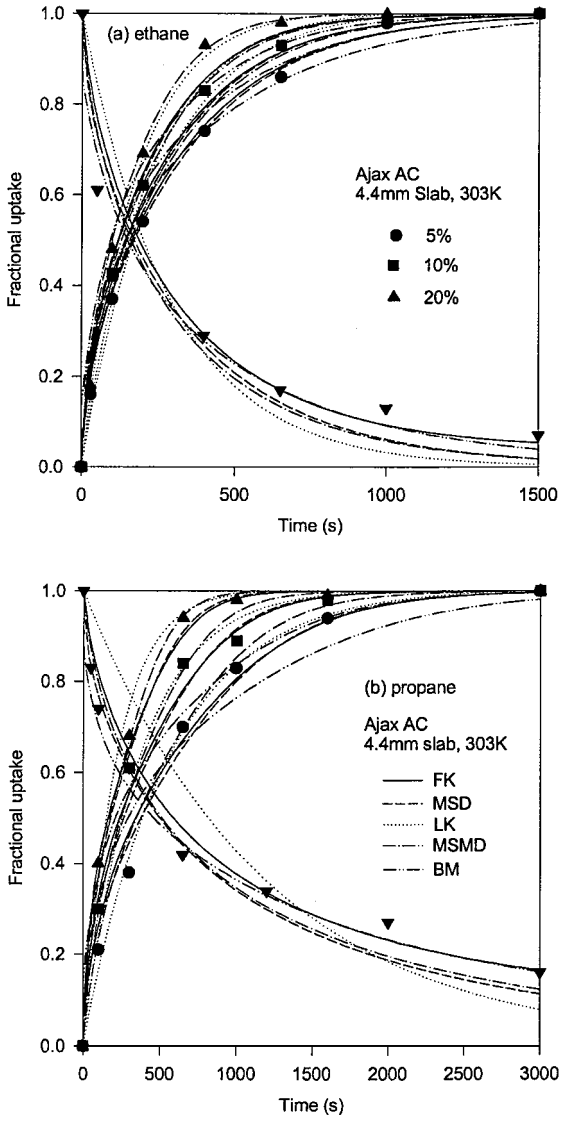


*Figure 1.* Model fittings/predictions and the experimental data of the two adsorbates on Ajax AC in 4.4 mm slab at 303 K. (a) Ethane, (b) propane (—— FK, – – – – MSD, · · · · · · LK, —·—·— MSMD, —·—·—·— BM).

i.e., MSD, MSMD, FK and LK perform well while the BM is inferior to the others.

With the derived kinetic parameters of each model, we compare the predictive capability of the MSD, MSMD, FK and BM models in simulating the pure component kinetics of ethane and propane on the Ajax sample at other two temperatures: 283 K and 333 K. At each temperature, three bulk phase composition, 5%, 10% and 20%, were simulated for each species. Since LK does not possess explicit temperature dependence, it is employed to *fit* the data at those experimental conditions. The AREs of the model prediction and fitting (LK) are listed in Table 4 for ethane and Table 5 for propane, respectively. We see that, as temperature changes, the MSD, MSMD, FK models present the correct temperature dependence. The LK model fits those data reasonably well. The prediction of BM model for propane, however, exhibits a larger deviation, indicating that its capability to predict kinetics at other temperatures is inferior to other models.

The model fittings (lines) and the experimental data (symbols) of ethane and propane on Norit AC in 8.82 mm slab at 303 K were shown in Fig. 2(a) and (b), respectively while the ARE of the fittings for each species are listed in Tables 6 and 7, respectively. The figures and the ARE show that the performance of each model are similar to those on Ajax AC, except that the fittings of LK are poor. The temperature dependence of each model are examined in the same procedures as those on Ajax AC, but with the kinetics data of each species measured at 333 K and 363 K and the bulk phase composition of 2%, 5% and 10%. The AREs for the predictions and fittings (LK) are shown in Tables 6 and 7 for ethane and propane, respectively. All the models present reasonable results for those two systems.

Next, the predictability the five models were compared by simulating the pure component desorption kinetics of ethane and propane on each AC sample. For Ajax AC, the temperature is 303 K and the bulk phase molar fraction is 10% for each species. The experimental data (symbols) and the model prediction (lines) are shown in Fig. 1(a) and (b), respectively. It is seen that FK and BM model give the best prediction results for those two systems. MSD and MSMD give reasonably predictions. LK predicts much faster kinetics although with the kinetics parameters derived from the same experimental temperature and bulk phase composition. The desorption kinetics of pure component ethane (5%) and propane (5%) on Norit AC in 8.82 mm slab at 303 K are also simulated. The experimental data (symbols) and the model predictions (lines) are shown graphically in Fig. 2(a) and (b) for ethane and propane, respectively. The prediction results of each model are consistent with those on Ajax AC.

It is seen that MSD, MSMD and FK model present reliable performance for each species at different operation mode. BM predicts the desorption data well but with relatively large deviations in fitting/predicting

*Table 4.* The kinetics parameters for ethane on the Ajax AC sample.

| | MSD | BM | LK | MSMD | | FK | |
|---|---|---|---|---|---|---|---|
| $D_p \times 10^6$ | $D_\mu^0$ | $D_{\mu 0}^*/r_0^2$ | $k_a \times 10^4$ | $D_\mu^0 \times 10^7$ | $r_0/\beta$ | $D_\mu^0 \times 10^7$ | $k_a \times 10^4$ |
| ($m^2/s$) | ($m^2/s \times 10^7$) | ($s^{-1} \times 10^2$) | (l/mol/$m^3$/s) | ($m^2/s$) | ($m \times 10^3$) | ($m^2/s$) | (l/mol/$m^3$/s) |
| 1.51, 1.68, 1.96 | 6.18 | 3.72 | 3.01, 2.78, 2.76 | 6.58 | 0.7 | 6.22 | 4.48 |
| ARE (%) | 6.10, 8.70, 7.00 | 10.6, 7.05, 4.84 | 5.64, 3.15, 7.88 | 5.14, 2.59, 6.50 | | 5.05, 6.15, 4.83 | |

Note: The values of $D_p$, LK, and ARE are in the order of temperatures, i.e., 283 K, 303 K and 333 K.

*Table 5.* The kinetics parameters for propane on the Ajax AC sample.

| | MSD | BM | LK | MSMD | | FK | |
|---|---|---|---|---|---|---|---|
| $D_p \times 10^6$ | $D_\mu^0$ | $D_{\mu 0}^*/r_0^2$ | $k_a \times 10^4$ | $D_\mu^0 \times 10^7$ | $r_0/\beta$ | $D_\mu^0 \times 10^7$ | $k_a \times 10^4$ |
| ($m^2/s$) | ($m^2/s \times 10^7$) | ($s^{-1} \times 10^2$) | (l/mol/$m^3$/s) | ($m^2/s$) | ($m \times 10^3$) | ($m^2/s$) | (l/mol/$m^3$/s) |
| 1.20, 1.30, 1.56 | 1.34 | 5.64 | 5.53, 4.63, 2.86 | 1.50 | 1.0 | 2.05 | 4.50 |
| ARE (%) | 4.55, 4.18, 4.70 | 10.7, 21.2, 29.2 | 4.50, 7.93, 7.49 | 3.62, 4.26, 7.52 | | 4.38, 5.18, 3.88 | |

Note: The values of $D_p$, LK, and ARE are in the order of temperatures, i.e., 283 K, 303 K and 333 K.

*Table 6.* The kinetics parameters for ethane on the Norit AC sample.

| | MSD | BM | LK | MSMD | | FK | |
|---|---|---|---|---|---|---|---|
| $D_p \times 10^6$ | $D_\mu^0$ | $D_{\mu 0}^*/r_0^2$ | $k_a \times 10^4$ | $D_\mu^0 \times 10^7$ | $r_0/\beta$ | $D_\mu^0 \times 10^7$ | $k_a \times 10^4$ |
| ($m^2/s$) | ($m^2/s \times 10^7$) | ($s^{-1} \times 10^2$) | (l/mol/$m^3$/s) | ($m^2/s$) | ($m \times 10^3$) | ($m^2/s$) | (l/mol/$m^3$/s) |
| 2.12, 2.26, 2.35 | 1.50 | 1.49 | 5.23, 4.38, 4.07 | 1.51 | 4.61 | 2.01 | 6.71 |
| ARE* (%) | 4.17, 4.99, 16.4 | 4.94, 4.39, 25.4 | 12.6, 9.31, 10.1 | 3.32, 3.50, 8.07 | | 4.03, 5.03, 16.3 | |

Note: The values of $D_p$, LK, and ARE are in the order of temperatures, i.e., 303 K, 333 K and 363 K.

*Table 7.* The kinetics parameters for propane on the Norit AC sample.

| | MSD | BM | LK | MSMD | | FK | |
|---|---|---|---|---|---|---|---|
| $D_p \times 10^6$ | $D_\mu^0$ | $D_{\mu 0}^*/r_0^2$ | $k_a \times 10^4$ | $D_\mu^0 \times 10^7$ | $r_0/\beta$ | $D_\mu^0 \times 10^7$ | $k_a \times 10^4$ |
| ($m^2/s$) | ($m^2/s \times 10^7$) | ($s^{-1} \times 10^2$) | (l/mol/$m^3$/s) | ($m^2/s$) | ($m \times 10^3$) | ($m^2/s$) | (l/mol/$m^3$/s) |
| 1.75, 1.86, 1.97 | 3.56 | 2.56 | 8.00, 6.55, 6.08 | 2.68 | 7.53 | 3.9 | 6.13 |
| ARE (%) | 4.63, 3.61, 4.40 | 7.70, 5.75, 6.29 | 9.58, 5.86, 5.07 | 4.90, 3.00, 3.62 | | 4.67, 3.61, 4.40 | |

Note: The values of $D_p$, LK, and ARE are in the order of temperatures, i.e., 303 K, 333 K and 363 K.

adsorption data. LK model fits the adsorption data reasonably well. However, this good fit results more from its mathematical flexibility rather than from its mass transfer mechanism, as the model poorly predicts the desorption data on ACs.

## 3. *The Adsorption Kinetics of Multicomponent Systems*

With the related kinetic parameters listed in Tables 4–7, the five models are employed to simulate the adsorption kinetics of binary ethane-propane systems on each AC sample. The adsorption kinetics of ethane (10%)–propane (10%) on Ajax AC in 4.4 mm slab pellets at 303 K were simulated first. The experimental data (symbols) and model simulation (lines) were shown in Fig. 3. It is seen that MSMD and MSD models correctly simulate the kinetics of each species. The LK model also amazingly gives a good prediction considering its mathematical simplicity. The FK model presents the next best prediction. The prediction of BM, however, presents a large deviation. The time and degree for the maximum overshooting of light species (ethane) are erroneously predicted.

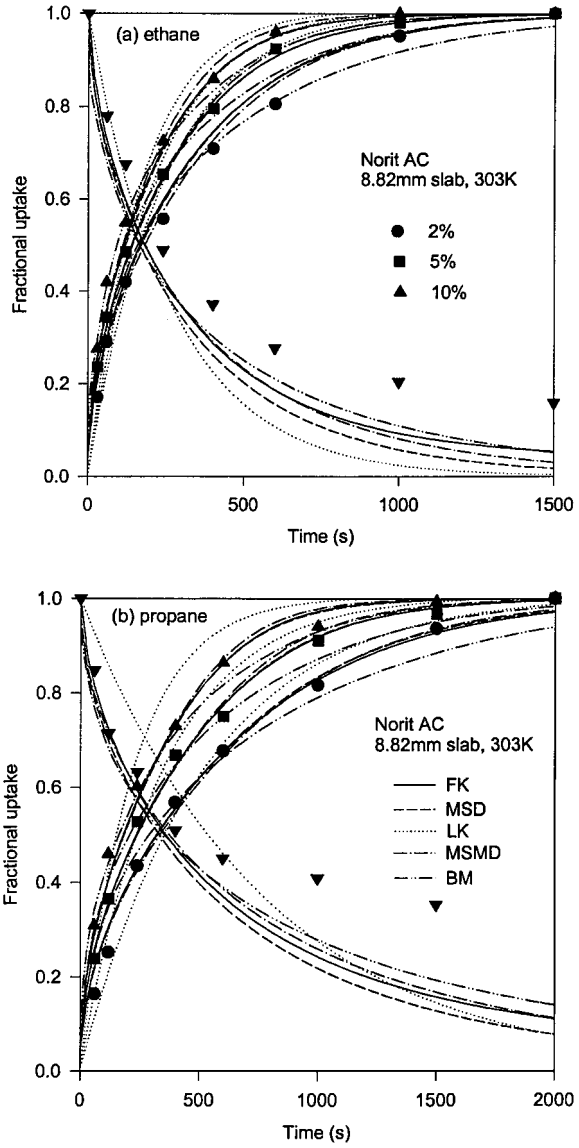


*Figure 2.* Model fittings/predictions and the experimental data of the two adsorbates on Norit AC in 8.82 mm slab at 303 K. (a) Ethane, (b) propane (——FK, – – – –MSD, · · · · · ·LK, –·–·– MSMD, –·–·–·–BM).

The adsorption kinetics of ethane (10%)–propane (10%) on Ajax AC in 4.4 mm slab at 333 K is then simulated with the five models. The experimental data (symbols) and the model predictions (lines) are compared in Fig. 4. Again, the MSD and MSMD models present good predictability and the FK model presents the next good predictability. LK exhibits some deviation for this system but is still more than qualitatively correct. BM again presents serious deviations.

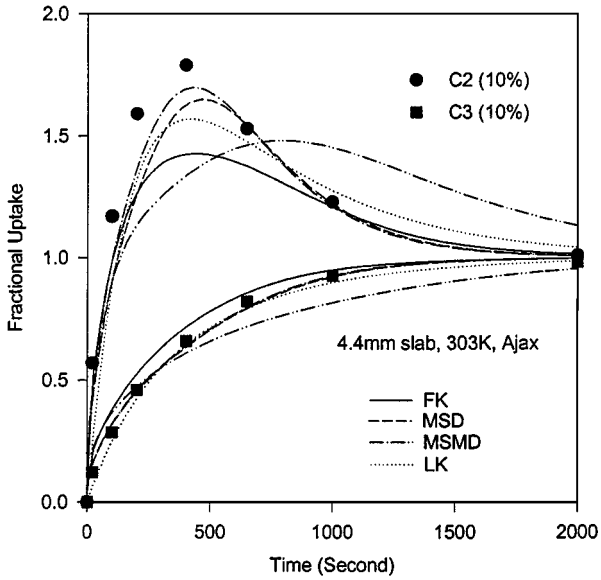


*Figure 3.* Model simulations and the adsorption kinetic data of the binary ethane (10%)–propane (10%) mixture on Ajax AC in 4.4 mm slab at 303 K. (——FK, – – – –MSD, · · · · · ·LK, –·–·– MSMD, –·–·–·–BM).

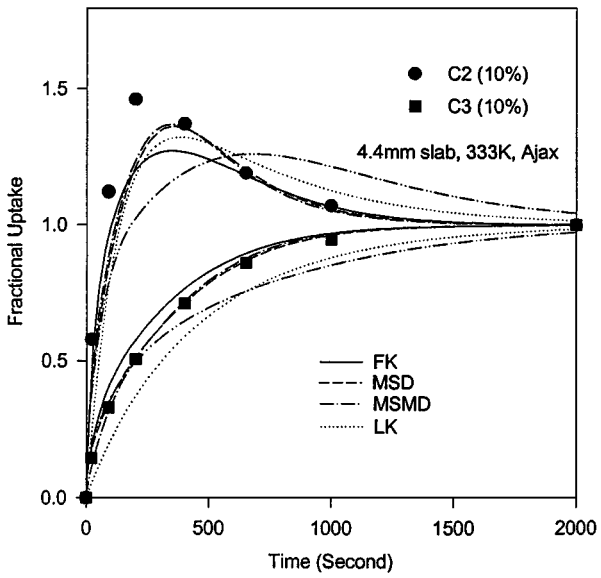


*Figure 4.* Model simulations and the adsorption kinetic data of the binary ethane (10%)–propane (10%) mixture on Ajax AC in 4.4 mm slab at 333 K. (——FK, – – – –MSD, · · · · · ·LK, –·–·– MSMD, –·–·–·–BM).

Next the co-desorption kinetics of ethane (10%)–propane (10%) on Ajax AC in 4.4 mm slab pellets at 303 K were simulated (Fig. 5). This time, the five models behave very differently. The model assuming

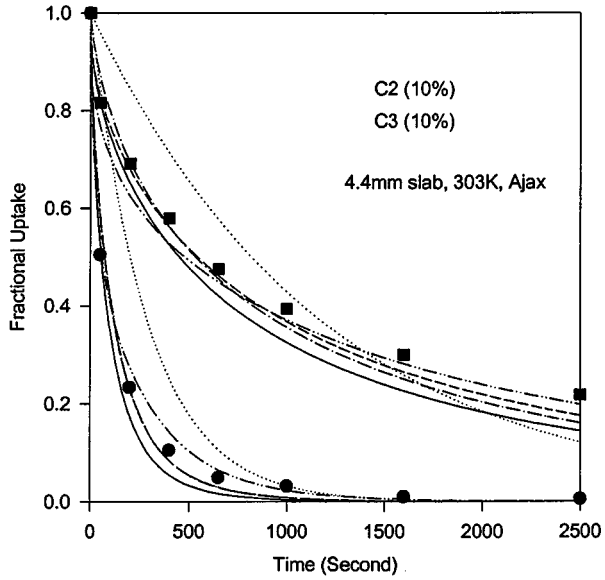


*Figure 5.* Model simulations and the desorption kinetic data of the binary ethane (10%)–propane (10%) mixture on Ajax AC in 4.4 mm slab at 303 K. (—— FK, – – – – MSD, · · · · · · LK, –·–·– MSMD, –·–·–·– BM).

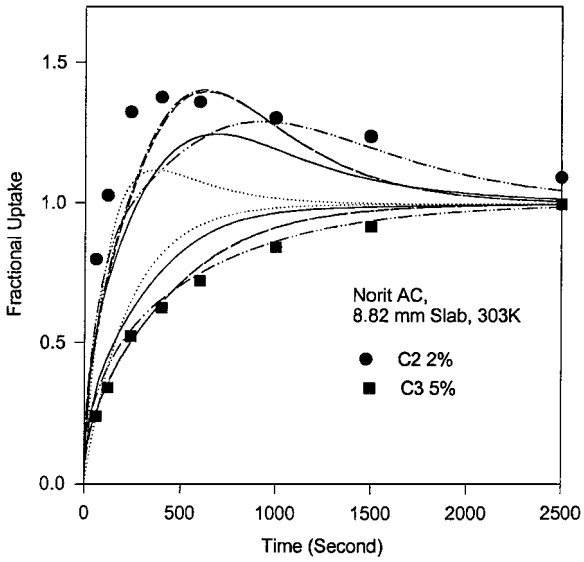


*Figure 6.* Model simulations and the adsorption kinetic data of the binary ethane (2%)–propane (5%) mixture on Norit AC in 8.82 mm slab at 303 K. (—— FK, – – – – MSD, · · · · · · LK, –·–·– MSMD, –·–·–·–0 BM).

surface flux along the particle scale, that is, the MSMD, MSD and FK models present comparable prediction results. The LK (the dashed lines) model fails to predict the kinetics of each species. The BM model gives the best predictions at long time, although it predicts a faster kinetics for propane at short time. This good prediction of BM at long time scale is understandable since the mass transfer resistance at long time is controlled by the ability of molecules leaving the micropores, which is well accounted for by the model.

Finally, three sets of sorption kinetic data of binary ethane–propane mixture on Norit AC in 8.82 mm slab pellets are simulated with each model. Figure 6 shows the model simulations (lines) and the experimental data (symbols) of binary ethane (2%)–propane (5%) on Norit AC at 303 K. We see that the FK model predicts a bit fast while the LK model predicts a much faster kinetics for this system. Figure 7 shows the prediction results of each model (lines) and the experimental data (symbols) of ethane (5%)–propane (5%) on Norit AC at 363 K. Figure 8 shows the simulation results of each model (lines) and the experimental data of the desorption kinetics of ethane (5%)–propane (5%) on Norit AC at 303 K. The performance of each model for these two systems are consistent with what we observed for Ajax AC.

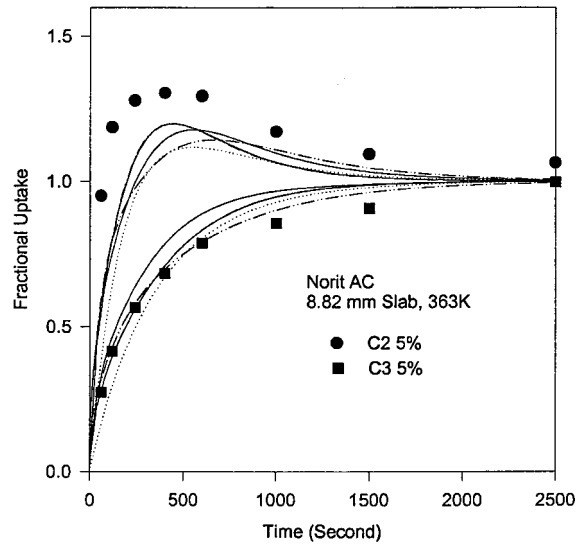


*Figure 7.* Model simulations and the adsorption kinetic data of the binary ethane (5%)–propane (5%) mixture on Norit AC in 8.82 mm slab at 333 K. (—— FK, – – – – MSD, · · · · · · LK, –·–·– MSMD, –·–·–·– BM).

## 4. *Discussion*

With the fitting and simulation results of each model in previous section, we can make some comments on their performance/applicability. Generally speaking, models

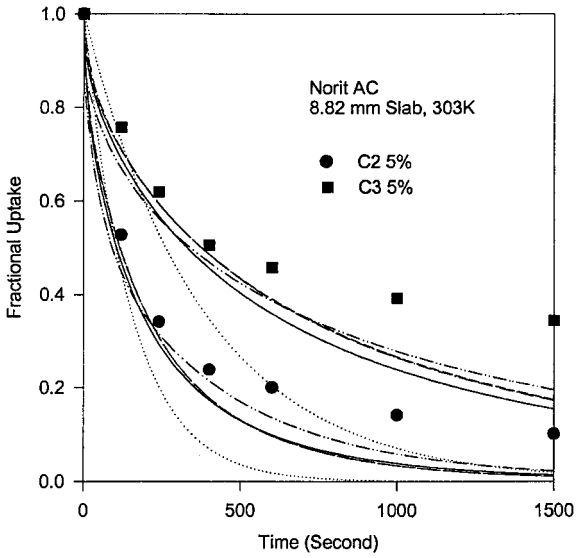


*Figure 8.* Model simulations and the desorption kinetic data of the binary ethane (5%)–propane (5%) mixture on Norit AC in 8.82 mm slab at 303 K. (—— FK, – – – – MSD, · · · · · · LK, —·—·— MSMD, —··—··— BM).

assuming diffusion flux along the particle scale (i.e., MSD, MSMD and FK) present better and stable performance for the pure as well as binary data, and within the three models the introduction of extra parameter (extra diffusion mechanisms) will not significantly improve the performance. This observation strongly supports the existence/importance of surface flux along the particle scale in ACs. The choice of a mathematical model for a particular sorption process may also depends on several other factors such as the purpose and the specific system. The simplicity may also be an important factor. The simplicity of the five model undoubted follows the order: LK $\gg$ MSD $\sim$ BM $>$ FK $>$ MSMD.

The MSD model assumes that the surface flux along particle scale is the only form of mass transfer in the adsorbed phase. This model is seen to present good consistency in fitting/predicting the pure as well as multicomponent kinetic data of ethane and propane on the two ACs. Together with its simplicity, the model constitutes the best choice for the description of the kinetics of likewise systems under various experimental conditions and operation modes. The MSD model can lead to, at least, the following conclusion: the assumption of diffusion flux along particle scale can effectively describe the sorption kinetics on ACs.

The MSMD model assumes the adsorbed phase diffusion along both particle and microparticle scales. The model performs better than MSD for kinetics on small particles (Du et al., 1991). On large sized particles, however, the improvement over MSD is insignificant. On the other hand, the model is disadvantaged by the extra fitting parameters and mathematical complexity. The convergence of MSMD model is also not as good as that of MSD. So for the systems in this study, the use of the MSMD is not recommended.

The FK model assumes an adsorbed phase flux along the particle scale and a finite mass interchange rate between the bulk and the adsorbed phases. It presents a good fit for pure component adsorption kinetics data and, especially, gives good prediction results for *desorption* kinetics of pure component systems. However, the prediction results for binary system are a bit inferior to MSD and MSMD. The performance of FK will likely improve if its original form is restored (Wang and Do, 1999) (that is, using the pore size distribution as the source of heterogeneity). The model has two unknown kinetics parameters and different combinations of these two parameters may affect the pure component kinetics and multicomponent kinetics differently (Wang and Do, 1999). The model's unsatisfactory prediction results for the binary kinetics on Norit AC may reflect this point, that is, the values of $K_a$ and $D_\mu$ of each species are not the optimal combination. This uncertainty is due to our insufficient understanding of the finite kinetics in AC. Thus, more fundamental research is needed to refine the model.

The LK model gives equivalently good fittings for pure component *adsorption* kinetics data and reasonably good predictions for binary *adsorption* kinetics data. Considering its simplicity, LK is a convenient substitute at the first approximation for simple systems involving only *adsorption* processes of which the temperature fluctuation is small. However, the good fit of LK is due to the mathematical flexibility rather than its correct description of the diffusion mechanism, since the model simply represents a first order differential equation. On the other hand, the model remarkably fails to predict *desorption* kinetics of the same system. This point is further strengthened when the model is compared with the binary desorption data.

BM model only fits some of the adsorption kinetics well. Although its prediction for the desorption kinetics are no inferior to other models, its predictability for multicomponent adsorption kinetics are much poorer. This model should not be used on ACs. The performance of BM indicates that the assumption of a sole

diffusion flux on microparticle scale is not consistent with the kinetic process on AC and can generate unsatisfactory fitting/simulation results.

## Conclusion

Five mathematical models with different mass transfer mechanisms are compared with the adsorption kinetics of pure as well as binary mixtures of ethane and propane on two AC samples. The results suggest that, on bidispersed AC samples, the role of the surface flux in the overall sorption kinetics is significant and needs to be properly addressed. The models fail to address the diffusion flux along particle scale, such as the BM and LK models, can possibly result in inferior prediction results or even serious deviation from the real experimental data. Especially, for system involving wide operating conditions and operated in various modes, the diffusion flux along particle scale can not be equivalently lumped/converted into the microparticle scale or shell resistance. However, for some simple systems, this requirement may be relaxed and only in this case BM or LK model may give equivalent results.

Among the models assuming the diffusion flux along the particle scale, MSD is the best choice with its stable performance and simplicity in formulation. The two-parametered MSMD model will not significantly improve the simulation/fitting results for large-sized particle. The FK (also two-parametered) model is valuable for the further investigation of diffusion mechanisms in ACs but needs to be further refined.

## Acknowledgment

Financial supports from the Croucher Foundation and the Research Grants Council of Hong Kong (Project No. HKUST6114/97P) and the support from the Australian Research Council are gratefully acknowledged.

## Nomenclature

| | |
|---|---|
| $a$ | ratio of activation energy for surface diffusion to adsorption energy |
| $b$ | adsorption isotherm parameter ($kPa^{-1}$) |
| BM | bimodal model |
| $C$ | bulk phase concentration ($kmol/m^3$) |
| $C_p$ | bulk phase concentration in macropore ($kmol/m^3$) |
| $C_0$ | initial bulk phase concentration ($kmol/m^3$) |
| $C_\mu$ | adsorbed phase concentration ($kmol/m^3$) |
| $C_{\mu 0}$ | initial adsorbed phase concentration ($kmol/m^3$) |
| $C_{\mu s}$ | saturation adsorption capacity ($kmol/m^3$) |
| $D_p$ | pore diffusivity ($m^2/s$) |
| $D_\mu$ | apparent surface diffusivity ($m^2/s$) |
| $D_\mu^0$ | surface diffusivity at zero energy level ($m^2/s$) |
| $E$ | local interaction energy (kJ/mol) |
| $E_a$ | activation energy for surface diffusion (kJ/mol) |
| F(E) | energy distribution function |
| FK | finite kinetics model |
| $J_P$ | diffusion flux in pore phase ($kmol/m^2/s$) |
| $J_\mu$ | diffusion flux in adsorbed phase along particle scale ($kmol/m^2/s$) |
| $J_\mu^r$ | diffusion flux in adsorbed phase along microparticle scale ($kmol/m^2/s$) |
| $k_a$ | adsorption rate constant ($1/mol/m^3/s$) |
| $k_d$ | desorption rate constant (1/s) |
| $k_m$ | mass transfer coefficient of film (1/s) |
| LK | Langmuir kinetics (model) |
| MSD | macropore and surface diffusion model |
| MSMD | macropore, surface and micropore diffusion model |
| $p$ | bulk phase pressure (kPa) |
| $R$ | particle scale (m) |
| $R_g$ | gas constant |
| $r$ | microparticle scale (m) |
| $s$, $s_\mu$ | geometric factor of particle, 0, 1, 2 for slab, cylinder and sphere |
| $t$ | time (s) |
| $\mu$ | chemical potential (J/mol) |
| $\varepsilon$ | porosity of adsorbent particle |

## References

Bhatia, S.K., "Transport in Bidispersed Adsorbents: Significance of the Macroscopic Adsorbate Flux," *Chem. Eng. Sci.*, **52**, 1377 (1997).

Do, D.D., "A Model for Surface Diffusion of Ethane and Propane in Activated Carbon," *Chem. Eng. Sci.*, **51**, 4145 (1996).

Do, D.D., "Dynamics of Adsorption in Heterogeneous Solids," *Equilibria and Dynamics of Gas Adsorption on Heterogeneous Solid Surfaces*, W. Rudzinski, W.A. Steele, and G. Zgrablich (Eds.), Elsevier, 1997.

Do, D.D. and K. Wang, "Dual Diffusion and Finite Mass Exchange Model for Adsorption Kinetics in Activated Carbon," *AIChE J.*, **44**(1), 68 (1998).

Do, D.D., X. Hu, and P.L.J. Mayfield, "Multicomponent Adsorption of Ethane, *n*-Butane and *n*-Pentane in Activated Carbon," *Gas Sep.*

*Purif.*, **5**, 35 (1991).

Gray, P.G. and D.D. Do, "Adsorption and Desorption of Gaseous Sorbates on a Bi-Dispersed Particles with Freundlich Isotherm III," *Gas Separ. Purif.*, **4**, 149 (1989).

Hu, X. and D.D. Do, "Multicomponent Adsorption Kinetics of Hydrocarbon onto Activated Carbon: Contribution of Micropore Resistance," *Chem. Eng. Sci.*, **48**, 1317 (1993).

Kapoor, A. and R.T. Yang, "Surface Diffusion on Energetically Heterogeneous Surfaces: An Effective Medium Approximation Approach," *AIChE J.*, **35**, 1735 (1989).

Kapoor, A. and R.T. Yang, "Contribution of Concentration-Dependent Surface Diffusion to Rate of Adsorption," *Chem. Eng. Sci.*, **46**, 1995 (1991).

Kapoor, A., R.T. Yang, and C. Wong, "Surface Diffusion," *Catal. Rev. Sci. Eng.*, **31**, 129 (1989).

Karger, J., "Mass Transfer Through Beds of Zeolite Crystals and the Paradox of the Evaporation Barrier," *Langmuir*, **4**, 1289 (1988).

Mann, R. and H.N.S. Yousef, "Interpretation of water isotherm hysteresis for an activated charcoal Using Stochastic Pore Networks," *Adsorption*, **1**, 253 (1995).

Prasetyo, I., and D.D. Do, "Adsorption Kinetics of Light Paraffins in AC by a Constant Molar Flow Rate Method," *AIChE J.*, **45**, 1892 (1999).

Qiao, S. and X. Hu, "Effect of Micropore Size Distribution Induced Heterogeneity on Binary Adsorption Kinetics of Hydrocarbons in Activated Carbon," *Chem. Eng. Sci.*, **55**, 1533 (2000).

Ruthven, D.M., *Principles of Adsorption and Adsorption Processes*, Wiley, New York, 1984.

Srinivasan, R., S.R. Auvil, and J.M. Schork, "Mass Transfer in Carbon Molecular Sieves—An Interpretation of Langmuir Kinetics," *Chem. Eng. J.*, **57**, 137 (1995).

Wang, K. and D.D. Do, "The Study of Multicomponent Adsorption, Desorption and Displacement Kinetics Using the Heterogeneous Finite Kinetics Model," *Separation & Purification Technology*, **17**, 131–146 (1999).